A Conformational Study of the Influence of Vibrations on Conduction in Molecular Wires

Maxine Olson, Yi Mao, Theresa Windus, Mathieu Kemp,* and Mark Ratner

Northwestern University, Department of Chemistry Evanston, Illinois 60208-3113

Natalia Léon and Vladimiro Mujica

Escuela de Química, Facultad de Ciencias Universidad Central de Venezuela, Apartado 47102, Caracas 1020A, Venezuela

Received: September 8, 1997; In Final Form: November 14, 1997

We present two examples of the influence of vibrations on electronic transport in molecular wires. Conductance is computed using a scattering approach and the effect of vibrations is included in a static picture where the conductance is computed for a sample of nuclear geometries. The physical picture involved is that of electrons tunneling elastically through variable geometries, and is a first approach to the real problem of inelastic scattering and dynamical electron−phonon coupling. The first example corresponds to a one-dimensional tight-binding model wire, where we study changes in conduction as a consequence of dimerization and soliton formation. In the second example, we consider a more realistic wire, a *p*-benzene-dithiol molecule, described with an extended Huckel Hamiltonian. We calculate the conductance for different distorted geometries obtained by taking displacements along the normal modes. For the tight-binding wire, we obtain important changes in the linear current depending on the location of the soliton deformation and the magnitude of dimerization. The effect is traced back to the strong influence geometry has on the electronic structure of the wire, whose overlap with the leads determines the current. For the *p*-benzene-dithiol case, we find a weak dependence of the effective coupling on the nature of the vibrational mode.

1. Introduction

Inelastic scattering is present in all electron transport processes in real systems, and is due to defect, electron−electron, and electron−phonon coupling.[1] Electron repulsion effects can be approximately included even at the one-particle level description (e.g., a Hartree−Fock treatment[2]), and different levels of accuracy in many-body treatments are available. The situation for the electron−phonon coupling is considerably more complicated, and not much has been done for real systems beyond the inclusion of linear coupling.[3]

Electron transfer is a common feature in many chemical reactions[4,5] and in conduction processes of the kind involved in scanning tunneling microscopy (STM) molecular imaging and mesoscopic devices containing molecular wires.[6] A reaction takes place when charge is transferred from a high-density center (the donor) to a relatively low-density center (the acceptor). In a nanoscopic device, charge is transferred between two macroscopic electrodes under the influence of an external electric field.

In both these cases, one can picture the transfer process as taking place through a vibrating molecular bridge. It is the change in nuclear conformation brought about by these vibrations, as well as their effect on the conductance, that will be considered in this article. The distinction between these vibrations and other nuclear displacement processes associated with the surrounding environment (usually a solvent) is particularly important for intramolecular electron transfer where solvent reorganization plays a crucial role in the description of the rate.[4]

A full quantum-dynamical approach to the problem would imply solving the Liouville−von Neumann equation for the density matrix of the system. Approximations including a finite number of phonon modes linearly coupled to the electrons (spin-boson model) have been made within the context of inelastic tunneling spectroscopy and also for electron-transfer (ET) reactions. A semiclassical treatment would imply treating classical nuclei coupled dynamically to the electronic systems. Related calculations using wave packet propagation in structureless potential barriers have been extensively used,[3,7−10] but little has been done for transfer in an actual molecular structure.

In this article, we will not consider dynamical electron−phonon coupling. Instead, a Born−Oppenheimer-like description will be used in which the transferred electrons tunnel through a molecular conformation where the positions of the nuclei correspond to a sample of the whole geometric manifold induced by the vibrations. This is equivalent to taking snapshots of the nuclear conformations. We then compute the current for each geometry. The physical rationale for this approach is clearly the assumption that the passage time of the electron through the bridge (analogous to the Landauer−Buttiker time[11]) is short compared to vibrational periods. Although this is an unsettled question about which there is much current arguing in the literature,[9−12] it seems clear that the residence time of a tunneling electron on a molecular bridge ($\sim 10^{-15}$ s) is rather short compared to the time involved in nuclear vibrations($\sim 10^{-12}$ s).

In section II of the article, we give a brief summary of the theory needed to compute the current. Section III examines the results, and section IV is devoted to a discussion of the results in the context of a more complete model for inelastic transfer processes.

S1089-5647(97)02940-4 CCC: $15.00
Published on Web 01/22/1998

2. Current in a Molecular Wire

We consider a device composed of a molecular wire M, coupled to two electrodes D (donor) and A (acceptor). Direct coupling between the electrodes is neglected (i.e., we consider only through-bond transport).

Our starting point is the expression for the linear current written as a sum of contributions of one-electron channels[13,14]

$$J_{\text{linear}}(E,W) = \frac{2\pi e^2}{\hbar} W \sum_{i,f} |\mathbf{T}_{fi}(E)|^2 \, \delta(E_i - E_{\text{F}}) \delta(E_f - E_F) = W\, g(E) \quad (1)$$

where W is the applied voltage, i and f denote the initial and final states in the donor and acceptor electrodes, E_{F} is the common Fermi energy of the reservoirs, E is the energy of the tunneling electron, and $\mathbf{T}$ is the transition matrix. $\mathbf{T}$ obeys the Lippmann−Schwinger equation[15]

$$\mathbf{T} = V + VGV \quad (2)$$

where V is the coupling between the electrodes and the wire and G is the Green's operator corresponding to the total Hamiltonian of the system H (i.e,

$$G(z) = (z - H)^{-1} \quad (3)$$

where z is a complex variable). Equation 1 also serves as the definition of the field-independent quantum linear conductance $g(E)$, which depends on the microscopic details of the wire-reservoir coupling and on the size of the wire.

The $\mathbf{T}$-operator in the Lippmann−Schwinger equation is, for nonrelativistic quantum mechanics, a two-body operator that connects n-body in- and out-states corresponding to times $t \rightarrow \pm\infty$. However, eq 1 corresponds to a one-electron approximation to the exact many-body current. Since we have neglected the direct coupling between the reservoirs, one can iterate the Lippmann−Schwinger equation and obtain in closed form:[13,14]

$$\mathbf{T}_{fi} = \sum_{k,k'} V_{f,k} G_{k,k'} V_{k',i} \quad (4)$$

where k and k' denote orbitals in the wire, which are assumed to be orthogonal.

Assuming that the electrodes are only coupled to the end sites in the wire (1 and N), eq 4 becomes

$$\mathbf{T}_{fi}(E) = V_{fN} G_{N1} V_{1i} \quad (5)$$

Insertion of this expression in eq 1 results in

$$g(E) = \frac{2\text{e}^2}{\pi\hbar} |G_{1N}|^2 \Delta_{\text{D}}(E_{\text{F}}) \Delta_{\text{A}}(E_{\text{F}}) \quad (6)$$

where the spectral density, $\Delta_K(E)$, K = D or A, associated to each reservoir is defined by

$$\Delta_K(E) = \pi \sum_p V_{Kp} \, \delta(E - E_{\text{p}}^{\text{o}}) \quad (7)$$

The calculation of $\Delta_K(E)$ depends on the model for the reservoir. As in refs 13 and 14, we use the Newns−Anderson chemisorption model.[16,17] This assumes that the metallic electrodes only couple to the atomic orbitals in direct contact with them. Defining V_{D} as the matrix element between site orbital D on the electrode and site 1 on the chain, the coupling between the metallic state k and site 1 on the chain is given by[16]

$$V_{k1} = V_{\text{D}} \sqrt{2/m + 1} \sin \theta_k \quad (8a)$$

where

$$\theta_k = k\pi/(m + 1), \, k = 1, 2, ..., m \quad (8b)$$

and m is the number of sites in the metal. A similar expression holds for the coupling at the other end of the wire. The tip itself can be considered as another site in the wire with a different site energy, since it is usually of the same material as the electrodes.

Using eqs 8, Newns[16] obtains a semielliptical $\Delta_K(E)$:

$$\Delta_{\text{K}}(E) = \left\{ \begin{matrix} \frac{V_K^2}{\gamma} \sqrt{1 - (E/2\gamma)^2} & |E/2\gamma < 1 \\ 0 & \text{otherwise} \end{matrix} \right\} \quad (9)$$

where E is now measured from the center of the energy band and 4γ is the reservoir energy bandwidth.

To put in a common framework previous results obtained for the tight-binding wire and a more general wire, it is convenient to write the Hamiltonian matrix for the donor−wire−acceptor system as

$$\mathbf{H} = \begin{bmatrix} \mathbf{H_E} & \mathbf{V_{EM}} \\ \mathbf{V_{ME}} & \mathbf{H_M} \end{bmatrix} \quad (10)$$

where $\mathbf{H_E}$ is an infinite diagonal matrix representing the electrode Hamiltonian, $\mathbf{H_M}$ corresponds to the wire, and $\mathbf{V_{EM}}$ is the electrode-wire interaction. Using the partitioning technique,[18−20] it is possible to include all effects of the electrodes in a reduced Green's function matrix of the same dimension as $\mathbf{H_M}$, whose elements are identical with those of the full Green's function as defined in eq 3

$$\mathbf{G}(z) = (z - \mathbf{H_M} - \Sigma)^{-1} \quad (11)$$

where $\mathbf{z}$ is a complex parameter and the matrix Σ represents the self-energy contributions due to the coupling to the continua of the electrodes. Σ is explicitly given by

$$\Sigma = \mathbf{V_{ME}} (z - \mathbf{H_E})^{-1} \mathbf{V_{EM}} \quad (12)$$

The matrix Σ has a complex expression, except when there is only coupling between one orbital in the wire and the electrode. For this case, as discussed in refs 2, 21, and 22, the only nonvanishing elements of Σ are $\Sigma_{11} \equiv \Sigma_1$ and $\Sigma_{NN} \equiv \Sigma_N$. They are given by

$$\Sigma_K(z) = \sum_p \frac{V_{Kp}^2}{\text{z} - \epsilon_p^{\text{o}}} = \Lambda_K(\epsilon) - \Delta_K(\epsilon), \quad K = 1 \text{ or } N; \quad p = i \text{ or } f \quad (13)$$

where ϵ_{p}o is the energy of the noninteracting states in the metal, and where Λ_K and Δ_K are respectively the real and imaginary parts of Σ. In the Newns−Anderson model,[16,17] Δ_K is given by eq 9, and Λ_K can be obtained as the Hilbert transform of Δ_K.

Although more general couplings between wires and electrodes can be treated numerically, we will keep the simple Newns' expression. Clearly the model has to be improved to include the possibility of multiple binding to the surface. This amounts to generalizing the self-energy matrix in eq 12, which

is a straightforward procedure to be done numerically. Steps in this direction have been taken in ref 21.

More important is the fact that our model depends strongly on the choice of donor and transfer orbitals, which is solely based on chemical intuition. This is a problem with all schemes based on orbital pictures, and one in which some progress can be expected if the theory is formulated consistently in terms of the electronic density. Work in this direction is in progress.

To define the effective coupling, we write the matrix $\mathbf{H_M}$ as

$$\mathbf{H_M} = \begin{bmatrix} H_D & H_{DA} & H_{D1} & H_{D2} & ... & H_{DM} \\ \mathrm{H_{AD}} & \mathrm{H_A} & H_{A1} & H_{A2} & ... & H_{AM} \\ H_{1D} & H_{1A} & H_{11} & H_{12} & ... & H_{1M} \\ H_{2D} & H_{2A} & H_{21} & H_{22} & ... & H_{2M} \\ \vdots & \vdots & \vdots & \vdots & ... & \vdots \\ H_{MD} & \mathrm{H_{MA}} & H_{M1} & H_{M2} & ... & H_{MM} \end{bmatrix} \quad (14)$$

where $M + 2$ is the number of orbitals in the wire, and two orbitals of the molecule (D and A) have been singled out to effectively carry all the coupling to the electrodes; that is, they play the roles of sites 1 and N in a one-dimensional chain.

Since atomic orbitals are in general nonorthogonal, the definition of the Green's function matrix for the wire must be modified accordingly:[23]

$$\mathbf{G}(z) = \mathbf{S}(z\mathbf{S} - \mathbf{H_M})^{-1}\mathbf{S} \quad (15)$$

where $\mathbf{S}$ is the overlap matrix. Equation 4 has to be correspondingly modified as

$$\mathbf{T}(z) = \mathbf{V}(z\mathbf{S} - \mathbf{H_M})^{-1}\mathbf{V} \quad (16)$$

In analogy with the tight-binding case, the G_{DA} element is computed as the corresponding element in the Green's function matrix of eq 15. Thereafter, the conductance is computed according to eq 6. The caveat with the partitioning technique we are using is that it implicitly assumes that reservoir and wire states are orthogonal to each other.

3. Results and Discussion

We present separately the results for the tight-binding and *p*-benzene-dithiol cases, where the current has been calculated according to eq 6 with the corresponding definitions for the relevant Green's function matrix elements.

3.1. Tight-Binding Wire: Peierls Distortion and Solitons. The tight-binding Hamiltonian for a chain with N sites is given by

$$H_{\mathrm{M}} = \sum_{i=1}^{N} \alpha_i |i\rangle\langle i| + \sum_{i=1}^{N-1} \beta_{i,i+1} |i\rangle\langle i+1| + CC \quad (17)$$

where the α's are the site energies, measured from the Fermi level of the electrodes, and the β's are the transfer integrals.

Dimerization and soliton formation are two closely related processes which have been extensively studied, first in the context of insulator−metal transition where dimerization is known as the Peierls instability[24] and later in the field of conducting organic polymers.[25] These two types of excitations appear as the combined effect of electronic correlation and electron−phonon coupling, and they play quite an important role in the transport dynamics and spectral properties of quasi-one-dimensional systems. In a one-dimensional chain, single-soliton formation can only take place if the chain has an odd number of sites.

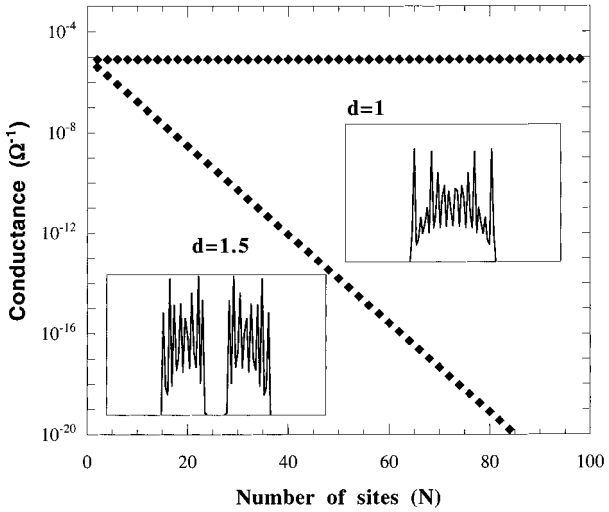

Figure 1. Length dependence of the conductance for two degrees of dimerization, for chains with an even number of sites. The injection energy is set at midgap, and the site−site coupling β_s is 0.1 eV. Without dimerization ($d = 1$), the conductance is length independent. With dimerization ($d = 1.5$), the conductance decreases exponentially with chain length. The insets show the opening of the gap for the dimerized chain.

Since the conduction is essentially a tunneling process across the molecular structure, it is sensitive to the density of states (DOS) at the tunneling energy.[26] Both dimerization and soliton formation modify dramatically the DOS, the former by creating an energy gap in the molecular band and the latter by creating new states in the band gap. The site-projected density of states (DOS) can be readily computed in terms of the Green's function as a function of the energy ϵ:

$$\omega_k(\epsilon) = -\frac{1}{\pi} Im(G_{kk}(\epsilon)), \quad \text{for} \qquad k = 1, ..., N \quad (18)$$

and the total DOS at ϵ is given by

$$\Omega(\epsilon) = \sum_{k=1}^{N} \omega_k(\epsilon) \quad (19)$$

Dimerization is introduced by considering two different values for the site−site interaction in the tight-binding Hamiltonian, one for double, β_{d}, and one for single bonds, β_{s}. They are related by $\beta_{\mathrm{d}} = d\beta_{\mathrm{s}}$, where d is a dimerization parameter. As discussed in refs 13 and 14, for a chain with the same value of α and β for all sites, the regime in which $\eta = \alpha/2\beta_{\mathrm{s}} < 1$ corresponds to the resonance condition in which the current (in the absence of bath coupling) does not decay with the distance between the electrodes; this is by far the most interesting case to study in molecular wires.

Figure 1 displays the current as a function of length, for chains with an even number of sites. Injection is taking place at midgap, and the current is shown for two values of the dimerization parameter. Increasing the dimerization by any amount translates into the appearance of a gap in the wire band whose magnitude is $2|(\beta_{\mathrm{d}} - \beta_{\mathrm{s}})|$. The presence of this gap destroys the resonance condition, and causes the current to decrease exponentially with distance. This is shown in the figure for the $d = 1.5$ case. It is clear that the critical change in DOS at the Fermi level (shown in the inset) is the main factor responsible for the different behavior of the undimerized and dimerized chains.

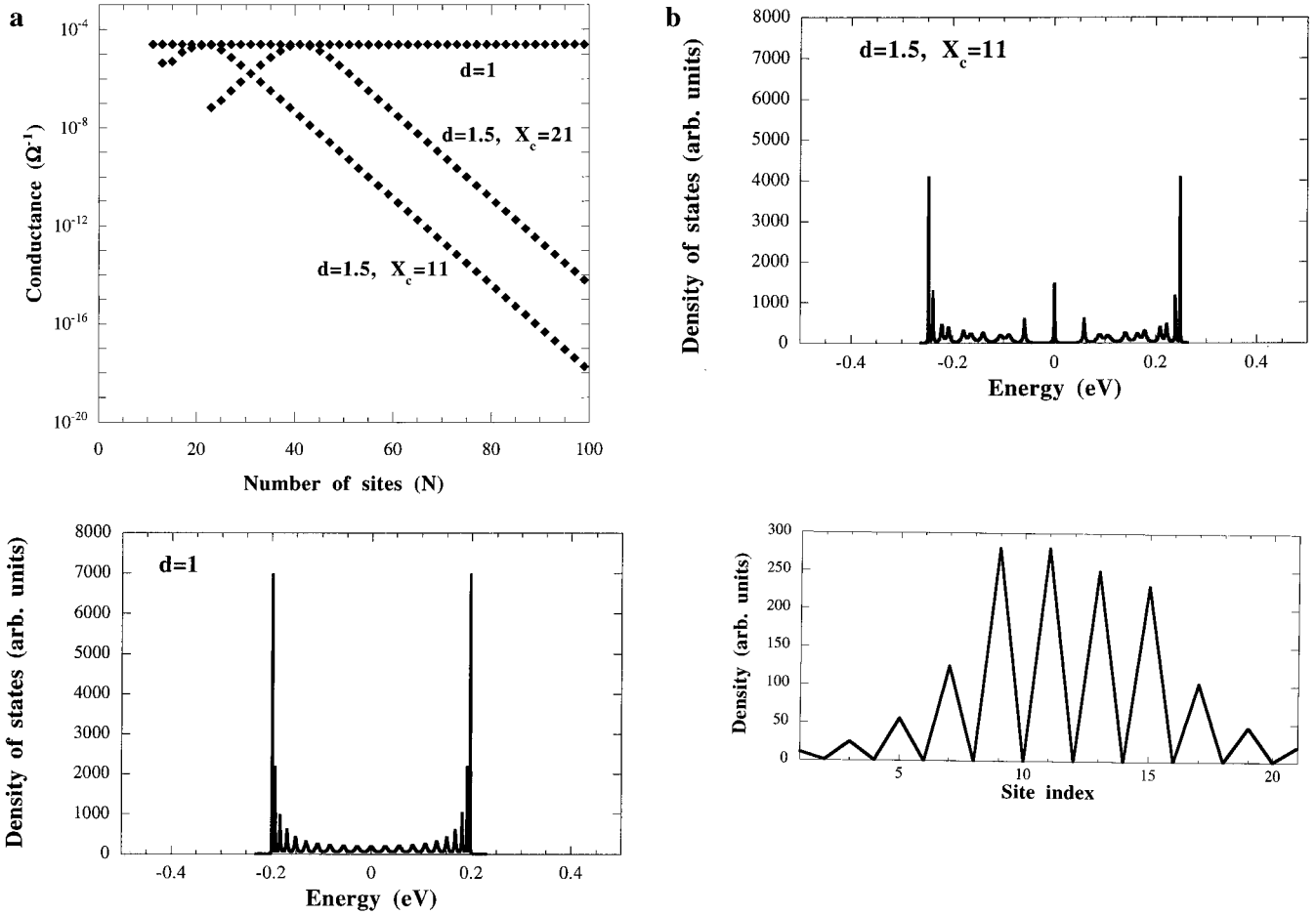

Figure 2. Length dependence of the conductance for two degrees of dimerization for chains with an odd number of sites and for a soliton length $S = 14$. In the dimerized case ($d = 1.5$), the kink is centered at two different positions ($X_c = 11$ and 21). The injection energy is set at midgap, and the site−site coupling β_s equals 0.1 eV. Without dimerization ($d = 1$), the conductance is length independent. With dimerization, the conductance increases with electrode-electrode distance for short chains, and decreases exponentially for long ones. The conductance also shows a strong dependence on the position of the soliton, increasing as the soliton moves toward the center of the chain. Figure 2b. Upper part: DOS for the undimerized and dimerized chain ($d = 1.5$). The presence of the soliton increases the midgap DOS. Lower part: Electronic site density for the ϕ_o molecular orbital, showing the localization pattern induced by the soliton kink.

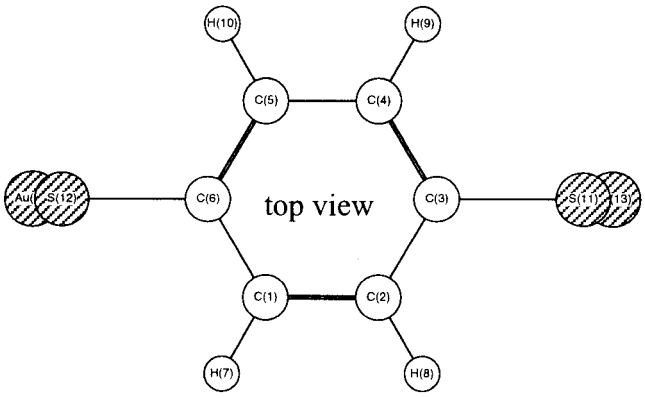

Figure 3. Top-view of the equilibrium molecule of the gold−(*p*-benzene-dithiol)−gold cluster used in the calculation of the conductance.

The simplest description of a soliton in an odd-numbered chain is as a topological deformation that appears in a dimerized, free radical chain. Around the position where the unpaired electron is, there is a mismatch in bond ordering. This mismatch is called a domain wall or topological soliton, and was found to be the variational solution of the Su−Schrieffer−Heeger Hamiltonian which is of the tight-binding form but includes an explicit expression for the electron−phonon interaction.[27−29]

A simple representation of the kink associated with the soliton is obtained by choosing an interpolation function that takes β from β_d to β_s (or vice versa) over a certain distance in the chain. An adequate interpolation function is the hyperbolic tangent[30,31]

$$\beta_{k,k+1} = \beta_s + \beta_o(1 + \tanh(x)) \qquad (20a)$$

$$\beta_{k,k+1} = \beta_d - \beta_o(1 + \tanh(x)) \qquad (20b)$$

where $-L < x < L$, $\beta_o = (\beta_d - \beta_s)/2$, and where eqs 20a,b give respectively the interpolation function from β_s to β_d and from β_d to β_s. The step in the variable x is taken equal to $4L/(N - 3)$, and L is defined as $L = 3N/S$, where S is the soliton length, which has been estimated to be around 14 sites.[28]

Figure 2a shows the resonance current as a function of distance for chains with an odd number of sites. Again, injection takes place at midgap. The current is shown for the undimerized chain, and for two soliton center positions. At large distances, the current exhibits the usual exponential dependence on distance. Surprisingly however, the current increases for short distances, reaching a maximum at $N = 2X_c$, where X_c is the position of the kink's center. In the dimerized case,

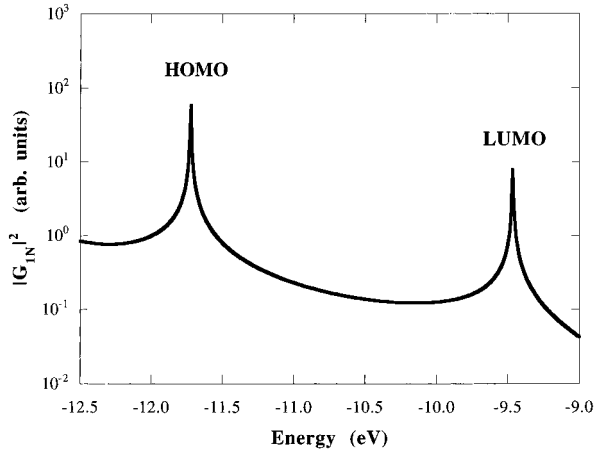

Figure 4. Energy dependence of the Green's function element G_{1N} for the molecule shown in Figure 3. The two peaks at −9.4 and −12.0 eV correspond to the HOMO and LUMO.

the current shows a very strong dependence on soliton position, increasing as the soliton moves toward the center of the wire.

Figure 2b compares the DOS for the chain with and without a soliton. Both cases have a midgap state. This state, denoted ϕ_o, is central to the conduction properties. In the undimerized case, ϕ_o is delocalized and connects the two electrodes. The presence of the kink modifies the localization pattern drastically, localizing the state at the position of the kink, thus increasing the midgap DOS.

The behavior of the current in the presence of the soliton can be understood in terms of a first-order perturbation expansion of the Green's function in eq 5. Assuming exponential localization of the state and keeping only the contribution arising from the ϕ_o orbital channel, we get

$$G_{1N} = \frac{1}{i}\frac{\langle 1|\phi_o\rangle\langle\phi_o|N\rangle}{\Delta_D|\langle 1|\phi_o\rangle|^2 + \Delta_A|\langle N|\phi_o\rangle|^2} \tag{21a}$$

which gives for the conductance:

$$g = \frac{1}{4\cosh^2[(N+1-2X_c)/\lambda]} \tag{21b}$$

where λ is the localization length of the soliton state.

Equation 21a shows that the behavior of the current is the result of the competition between two factors: (1) the mixing of the soliton state with the reservoirs, shown by the denominator, and (2) the overlap between the soliton state and the two reservoirs, shown by the numerator. For short distances, the mixing decreases faster with distance than the overlap, causing an increase in current. For larger distances, the mixing becomes minimal, but the overlap decreases exponentially, producing exponential decay.[32]

3.2. *p*-Benzene-Dithiol Wire. The computation of the current requires that the Hamiltonian matrix of the molecule be known. We use the extended Hückel model to calculate the electronic structure once the geometry of the molecule is known. In this model, the nondiagonal matrix elements of the Hamiltonian are given by the Wolfsberg−Helmholtz approximation[33]

$$H_{i,j} = KS_{i,j}\frac{H_{ii}+H_{jj}}{2} \tag{22}$$

where H_{ii} are the site energies, S_{ij} is the overlap matrix element which depends on the geometry, and K is a constant (here chosen as 1.75).

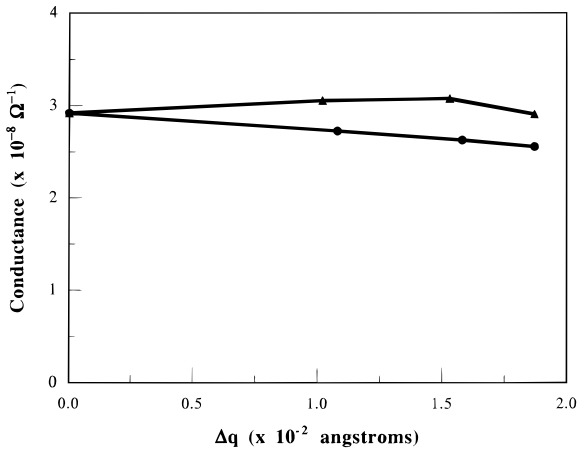

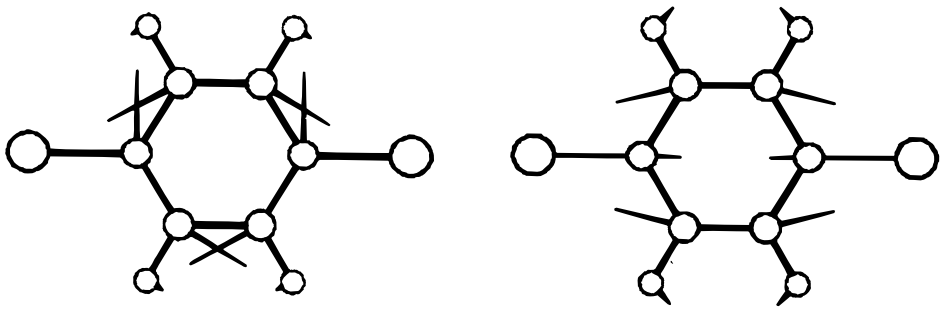

Figure 5. Dependence of the conductance on the displacement for selected normal modes. The modes are shown in Figure 5b. The upper (lower) part of Figure 5a corresponds to the upper (lower) part of Figure 5b.

The geometry itself is determined by energy optimization using GAUSSIAN 92,[34] which is also used to perform the normal modes analysis for the molecule. To model the wire attached to two electrodes and to determine the equilibrium geometry, we consider a complex formed by the molecule and two gold atoms. The equilibrium geometry is depicted in Figure 3. The gold atoms are necessary for the optimization of a geometry that preserves the conjugated character and the planarity of the phenyl ring. The chemisorption interaction of the wire with the surface of the electrodes is however treated within the Newns−Anderson model as explained in section II.

A crucial step in calculating the conductance is the determination of the position of the metal Fermi level with respect to the molecular band. We assume that the Fermi level lies in the middle of the molecular HOMO−LUMO gap,[21] which seems to be consistent with experimental evidence for wires and semiconductors. To take into account the electrostatics of the problem would require solving self-consistently the Poisson and Schrödinger equations. We have recently made progress in this direction and the results will be published elsewhere.

Figure 4 shows a plot of $G_{DA}(\epsilon)$ as a function of the injection energy ϵ at the equilibrium geometry. The value of V_K/γ in eq 9 was taken to be 0.1, which for a typical metal (4γ around 10 eV) corresponds to an adsorbate−surface interaction strength of around 1 eV. The figure shows resonance peaks at approximately −9.4 and −12.0 eV, corresponding to the LUMO and HOMO, respectively. The Fermi level is taken at midgap, which gives for $\log[|G_{DA}|]$ a value of −2.22 and a conductance of $3 \times 10^{-7}\ \Omega^{-1}$.

We construct the geometry modification induced by the vibrations the following way: At a given temperature, we use the equipartition theorem to compute a typical value of displacement around the equilibrium position, Δq_λ involved in a normal mode q_λ; that is, we set

$$\Delta q_\lambda = \sqrt{\frac{k_B T}{k_\lambda}} \tag{23}$$

where k_λ is the force constant of the mode. The Cartesian displacements Δr_i are then computed according to

$$\Delta r_i = c_{i\lambda} \Delta q_\lambda \tag{24}$$

where the $c_{i\lambda}$ are the elements of the rotation matrix between the normal (λ) and Cartesian displacements i. Once the Cartesian displacements are known, they are added to the original Cartesian coordinates of the molecule with the optimal geometry. This new geometry is then used as input for the extended-Hückel code and the current is recomputed. The approach we are following consists of assessing the effect of each mode separately on the current. A more complete treatment of the temperature dependence however would call for temperature sampling over all the modes.

A convenient way to express the variation in conductance for the different modes, is to compute the conductance derivative $\Delta g/\Delta\ q_\lambda$, where Δg is the difference in wire conductances at equilibrium and at the displaced geometry in the λth mode. Although it is difficult to establish a general trend in the results, there are several noteworthy features which are examplified in Figure 5. First, in general variations in conductance are on the order of 1% in the range of 0−300 K. There are, however some modes, where variations are on the order of 5%. Second, large negative variations invariably involve motion of the hydrogen atoms whereas the positive ones seem to be associated with C−C and C−S stretch. Somewhat surprisingly, based on the expectation that it would contribute to a decrease in conjugation along the wire, out-of-plane bending of the molecule does not affect the conductance in any significant amount.

4. Conclusions

We have studied two examples of the interplay between molecular vibrations and electronic conduction across a molecular wire. In the first case, we assume that vibronic coupling produces a soliton kink in the molecule, and inject an electron through it. This is an instance of off-diagonal disorder which differs considerably from the diagonal case.[35] We find that for short chains, the conductance increases with length, and that for long ones it decreases exponentially with distance. This behavior is due to the competition between the mixing of the soliton state and its overlap with the reservoirs. We also find that the conductance strongly depends on the position of the soliton kink, which in real systems might produce strong observable dynamical fluctuations of the current.

In the second case, we inject an electron on a *p*-benzenedithiol molecule distorted along its various normal modes of vibration. We find that, because of the relative rigidity of the molecule, the deformations induced by the vibrations induce little change in the current. This conclusion depends strongly on the assumption that the electrode's Fermi energy lies in the HOMO−LUMO gap. For injection energies close to wire energy levels, the conductance is expected to exhibit important variations.

Acknowledgment. Collaboration between Caracas and Evanston is supported by NSF and CONICIT. We are also grateful to the Chemistry Divisions of the NSF and ONR for partial support.

References and Notes

(1) Perrson, B. N. J.; Baratoff, A. *Phys. Rev. Lett.* **1987**, *59*, 339.
(2) Mujica, V.; Kemp, M.; Roitberg, A.; Ratner, M. A. *J. Chem. Phys.* **1996**, *104*, 7296.
(3) Vekhter, B. G.; Ratner, M. A. *J. Chem. Phys.* **1994**, *101*, 9710.
(4) Marcus. R. A.; Sutin, N. *Biochim. Biophys. Acta* **1985**, *811*, 265.
(5) Newton, M. D.; Sutin, N. *Annu. Rev. Phys. Chem.* **1984**, *35*, 437.
(6) For example, see: (a) *Molecular Electronics Science and Technology*; Aviram, A., Ed.; Washington, DC, 1992. (b) Jortner, J., Ratner, M. A., Eds; Blackwells, London, 1997. *Molecular Electronics*. (c) Reed, M.; Zhou, C.; Muller, C.; Burgin, T.; Tour, J. *Science* **1997**, in press. (d) Dhirani, A.; Liu, P.; Guyot-Sionnest, P.; Zehner, R.; Sita, L. *J. Chem. Phys.* **1997,** *106*, 5249. (e) Reimers, J. R.; Hush, N. S. *J. Photochem. Photobiol*. **1994**, *A 82*, 31. (f) Joachim, C.; Gimzewski, J.; Schlitter, R.; Chavy, C. *Phys. Rev. Lett.* **1995**, *74*, 2102. (g) Joachim C.; Vinuesa, J. F. *Europhys. Lett.* **1996**, *33*, 635. (h) Joachim, C.; Sautet, P. In *Scanning Tunneling Microscopy and Related Methods*; Behm, R. J., Garcia, N., Rohrer, H., Eds.; Kluwer Academic: Dordrecht, 1990.
(7) Billing, G. D.; Mikkelsen, K. V. *Chemical Dynamics and Reaction Kinetics*; Academic: New York, 1997; Vol. 2.
(8) Stövneng, J. A.; Hauge, E. H.; Lipavsky, P.; Spicka, V. *Phys. Rev. B* **1991,** *44*, 13595.
(9) Collins, S.; Lowe, D.; Barker, J. R. *J. Phys. C* **1987**, *20*, 6213.
(10) Hauge, E. H.; Stövneng, J. A. *Rev. Mod. Phys.* **1989**, *61*, 917.
(11) Büttiker, M.; Landauer, R. *Phys. Rev. Lett.* **1982**, *49*, 1739.
(12) Hagmann, M. G. *Int. J. Quantum Chem.* **1992**, *S 26*, 299.
(13) Mujica, V.; Kemp, M.; Ratner, M. A. *J. Chem. Phys.* **1994**, *101*, 6894.
(14) Mujica, V.; Kemp, M.; Ratner, M. A. *J. Chem. Phys.* **1994**, *101*, 6856.
(15) Taylor, J. R. *Scattering Theory*; Wiley: New York, 1972.
(16) Newns, D. M. *Phys. Rev.* **1969**, *178*, 1123.
(17) Anderson, P. W. *Phys. Rev.* **1961**, *124*, 41.
(18) Löwdin, P. O. *J. Math. Phys*. **1962**, *3*, 969.
(19) Evenson, J.; Karplus, M. *J. Chem. Phys.* **1992**, *96*, 5272.
(20) Sautet, P.; Joachim, C. *Chem. Phys. Lett.* **1988**, *153*, 511.
(21) Samanta, M. P.; Tian, W.; Datta, S.; Henderson, J. I.; Kubiak, C. P. *Phys. Rev. B* **1996**, *53*, R7626.

(22) Datta, S. *Electronic Transport in Mesoscopic Systems*; Cambridge University Press: Cambridge, 1995.

(23) Priyadarshy, S.; Skourtis, S. S.; Risser, S. M.; Beratan, D. N. *J. Chem. Phys.* **1996**, *104*, 9473.

(24) Peierls, R. E. *Quantum Theory of Solids*; Clarendon Press: Oxford, 1955.

(25) Conwell, E. M. In *Semiconductors and Semimetals*; Academic Press: Dordrecht, 1988; Vol. 27.

(26) Filali-Mouhim, A.; Lopez-Castillo, J.; Plante, I.; Jay-Gerin, J. P. *J. Phys. Chem.* **1996,** *100*, 12311.

(27) Pople, J. A.; Walmsley, S. H. *Mol. Phys.* **1962**, *5*, 15.

(28) Su, W. P.; Schrieffer, J. R.; Heeger, A. J. *Phys. Rev. B* **1980**, *22*, 2099.

(29) André, J. M.; Delhalle, J.; Brédas, J. L. *Quantum Chemistry Aided Design of Organic Polymers*; World Scientific: Singapore, 1991; Vol. 2.

(30) Mujica, V.; Correia, N.; Goscinski, O. *Phys. Rev. B* **1985**, *32*, 4178.

(31) Mujica, V.; Correia, N.; Goscinski, O. *Phys. Rev. B* **1985**, *32*, 4186.

(32) Magoga, M.; Joachim, C. *Phys. Rev. B* **1997**, *56*, 4722.

(33) Wolfsberg, M.; Helmholtz, L. *J. Chem. Phys.* **1952**, *20*, 837.

(34) Ab initio calculations were carried out using the Gaussian 92 series of programs: Frisch, M. J.; Trucks, G. W.; Head-Gordon, M.; Gill, P. M. W.; Wong, M. W.; Foresman, J. B.; Johnson, B. G.; Schlegel, H. B.; Robb, M. A.; Replogle, E. S.; Gomperts, R.; Andres, J. L.; Raghavachari, K.; Binkley, J. S.; Gonzalez, C.; Martin, R. L.; Fox, D. J.; Baker, J.; Stewart, J. J. P.; Pople, J. A. Gaussian, Inc.: Pittsburgh, PA, 1992.

(35) Economou, E. N.; Antoniou, P. D. *Solid State Commun.* **1977**, *21*, 285. Weaire, D.; Srivastava, V. *Solid State Commun.* **1977**, *23*, 863. Odagaki, T. *Solid State Commun.* **1980**, *33*, 861.